

Chapter 3

Mechanism and Modeling of Ring Pattern Formation for Electron Beam Exposure on Zwitterresist

Abstract

The novel sensitivity curve was determined for the zwitterresist. The irradiation dose in the center could create a ring pattern due to simultaneous exhibition of the positive tone and negative tone of zwitterresist. The natural logarithm dependence of ring width and electron beam dose was linear in two ranges, irrespective of the dot design radius. The heating effect was identified from $600 \mu\text{C}/\text{cm}^2$, while it could be neglected at less than $600 \mu\text{C}/\text{cm}^2$. Mathematical modeling for the prediction of ring width for zwitterresist was achieved by considering the electron scattering and heating effects. The results of experimental measurement and modeling on ring width showed a very good correlation. [DOI: 10.1143/JJAP.42.3838]

3.1 INTRODUCTION

The mask for the 130 nm design rule for optical lithography will cost up to three times that for the 180 nm design rule.[1] Small-volume production is not suitable for optical lithography for less than 130 nm design due to the high mask cost. Hence, the electron beam writing technology will have a cost advantage for production volumes below 100 lots in the future.[2] The use of zwitterresist for electron beam technology has been reported to increase the throughput.[3] A zwitterresist refers to a resist, which depending on the applied doses, can exhibit a positive tone and a negative tone. The technology of simultaneous positive tone and negative tone patterning will be beneficial for the application of electron beam direct writing technology in the future.[3]

The strategy of saving writing time in the case of electron beam direct writing is depicted in Figure 3-1. The positive resist is suitable for patterning contact holes or high density patterns, while the negative resist is suitable for patterning gate or low density pattern. The writing strategy will be confusing, if the same layer contains both high-density and low-density patterns. Therefore, the development of the zwitterresist process can be used to avoid the problem of writing confusion.

In electron beam writing, scattering effects such as forward scattering or backscattering can seriously affect design features due to electron proximity. [4] Moreover, a high electron dosage can create a thermal effect on the resist in addition to the scattering effect. In this study, the effect of dose and design radius on the ring pattern dimension is evaluated. The resultant pattern dimension of the zwitterresist layer is characterized, and the model for predicting the ring width is established. Furthermore, the scattering and heating effects of the electron beam are identified and discussed based on experimental results.

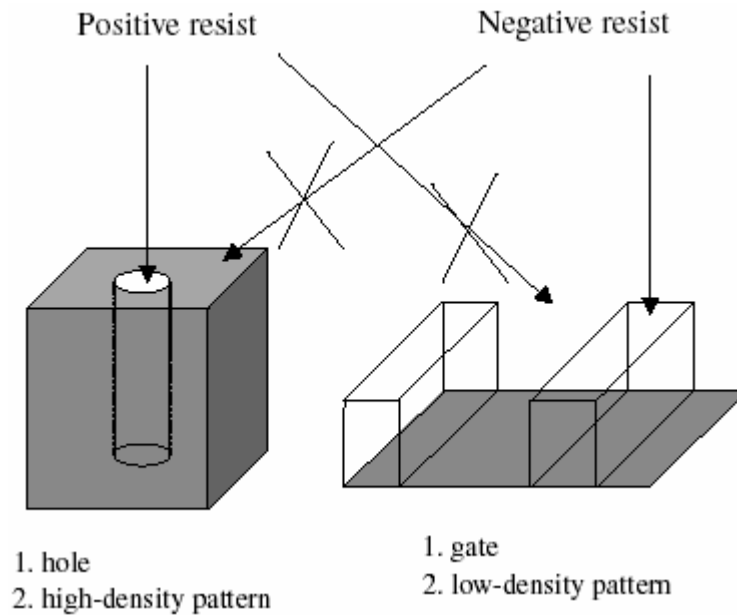


Figure 3-1. Strategies for electron beam direct writing.

3.2 EXPERIMENT

The chemical amplified ArF photoresist, obtained from Sumitomo Chemical Company (Tokyo, Japan) was used for electron beam exposure. The ingredients of the resist were 45–60% propylene glycol monomethyl ether acetate, 30–40% ethyl lactate, 5–20% acrylic resin and <1% acid generator. Electron beam exposure was carried out on a Leica Weprint model-200 stepper (Jena, Germany). The electron beam energy was 40 kV with beam size of 20 nm and beam current of 40 A/cm². The developer (AD-10) used was an aqueous solution containing 2.38% tetramethylammonium hydroxide (TMAH), and was obtained from Kemitek Industrial Corp., Taiwan. Pattern dimension was evaluated using in-line scanning electron microscope (SEM, Hitachi S-6280H, Tokyo, Japan).

3.3 RESULTS AND DISCUSSION

3.3.1 Sensitivity Curve and Formation of Ring Pattern

The sensitivity curve for irradiation doses on positive ArF resist is illustrated in Figure 3-2. The irradiating dose is concentrated in the central area. The zwitterresist in the center is affected by higher electron doses ($>300 \mu\text{C}/\text{cm}^2$), and the resist changes into a negative tone one (i.e., the circular pattern of S_1 area in Figure 3-2). On the contrary, the S_2 and S_3 areas only receive the scattering electrons from the S_1 area. In the S_2 area, the dose is estimated in the range of $3-300 \mu\text{C}/\text{cm}^2$. Hence, the resist maintains the positive tone behavior (i.e., ring pattern of S_2 area in Figure 3-2). In the S_3 area, the lower electron dose ($<3 \mu\text{C}/\text{cm}^2$) has no effect on resist reaction. The formation of a ring pattern (S_2 area) between S_1 area and S_3 area can reflect the specific characteristics of zwitterresist.

3.3.2 Influence of Electron Scattering Effect and Electron Heating Effect

Figure 3-3 reveals the relationship between the applied electron dose and the obtained ring width ($= r_2 - r_1$) at various design dot radiuses ($= r_1$). It is interesting that the natural logarithm relationship between ring width and electron dose less than $600 \mu\text{C}/\text{cm}^2$ behaves linearly. In addition, it also exhibits a higher and linear slope after a $600 \mu\text{C}/\text{cm}^2$ dose. In Figure 3-3 (a), these slopes are the same (i.e., 0.15) as those before the $600 \mu\text{C}/\text{cm}^2$ dose. Also, these slopes in Figure 3-3 (b) are close to 0.25.

In general, the scattering effect has a linear relationship with the natural logarithm of the dose. However, the experimental results, as shown in Figure 3-3, do not follow this prediction. This finding implies other factors maybe involved in the electron writing in addition to the electron scattering. Figure 3-4 depicts the electron

scattering effect and heating effect with respect to electron dose. In the lower dose region, only electron scattering can affect the design dimension. In the higher dose region, the heating from the central area (S_1) cannot be neglected in addition to the scattering effect. The heating also induces the reaction of chemical bonding, and increases the ring width. As a result, the ring width abruptly increases with dose from $600 \mu\text{C}/\text{cm}^2$ (ln 600=6:4).

3.3.3 Modeling the Effect of Electron Beam Dose

As mentioned above, the ring width ($D = r_2 - r_1$) is influenced by electron scattering effect and electron heating effect. Based on the observation of Figures 3-3 and 3-4, the electron scattering effect can be separated from the electron heating effect. The semi-empirical model for explaining the scattering and heating effects with respect to ring width is given as

$$D = k_s (E/\rho_s)^{\alpha_s} * k_h (E/\rho_h)^{\alpha_h} \quad (1)$$

Equation (1) can be expressed as

$$\ln D = \ln k_s + \ln k_h + \alpha_s (\ln E - \ln \rho_s) + \alpha_h (\ln E - \ln \rho_h) \quad (2)$$

where D is ring width, E is electron dose, k and α are coefficients, the subscript s denotes scattering effect, and the subscript h denotes heating effect. ρ is the coefficient of unit transformation. Based on the results in Figures 3-3 and 3-4, the heating effect can be neglected at a dose of less than $600 \mu\text{C}/\text{cm}^2$. Hence, eq. (2) can be rewritten as eq. (3).

$$\ln D = \ln K_s + \alpha_s \ln E, E < 600 \mu\text{C}/\text{cm}^2 \quad (3)$$

where $K_s = k_s/\rho_s^{\alpha_s}$ and $K_h = k_h/\rho_h^{\alpha_h}$. Also, eq. (2) can be rewritten as eq. (4) for dose higher than $600 \mu\text{C}/\text{cm}^2$.

$$\ln D = \ln K_s + \ln K_h + \alpha_s \ln E + \alpha_h \ln E, \quad E > 600 \mu\text{C}/\text{cm}^2 \quad (4)$$

The α_s and $\ln K_s$ in eq. (3) can be solved due to the linearity of $\ln D$ versus $\ln E$ in Figure 3-3 within a dose of $600 \mu\text{C}/\text{cm}^2$, irrespective of design radius (i.e., r_1). As listed in Table 3-1, α_s is a constant, whereas $\ln K_s$ behaves as a function of natural logarithm on design radius (r_1). Inserting α_s from Table 3-1 into eq. (4) at an electron dose E , yields:

$$\ln D - \ln K_s - \alpha_s \ln E = \ln \left(\frac{D}{K_s E^{\alpha_s}} \right) = \ln K_h + \alpha_h \ln E, \quad E > 600 \mu\text{C}/\text{cm}^2 \quad (5)$$

Equation (5) indicates that the scattering effect is subtracted from the total electron effect, and the relationship of heating effect ($\ln D - \ln K_s - \alpha_s \ln E$) and $\ln E$ is still linear. Therefore, α_h and $\ln K_h$ can be extracted. Figure 3-5 depicts the α_h and $\ln K_h$ at any design radius of interest. The α_h increases linearly with natural logarithm of design radius (r_1), while $\ln K_h$ decreases linearly with natural logarithm of design radius (r_1). This observation suggests that the coefficients of electron heating effect can be expressed as a function of design radius (r_1).

By incorporating the coefficients of electron scattering and heating in Table 3-1 into eqs. (3) and (4), the mathematical models of electron dosing effect on zwitterresist ring width ($D = r_2 - r_1$) can be summarized as shown in Table 3-1. The semi-empirical model can be used to predict the ring width (D) under various electron doses (E) and design radiuses (r_1). To validate the model, the experimental measurements on ring width were compared with the model predictions, as shown in

Figure 3-6. Evidently, excellent agreement between the experimental results and the model's prediction ($r^2 \approx 0.99$) was observed for different sets of electron beam exposure on zwitterresist.

3.3.4 Throughout Calculation

To realize the throughout of zwitterresist in the application of IC design, a 2 cm×1 cm rectangle was used as a testing pattern. The rectangle was divided two parts of a 1 cm×1 cm square as shown in Figure 3-7 (a). The 2 μm×100 μm line patterns was used as negative tone testing patterns in one 1cm×1cm square and hole patterns with 1 mm radius were used as positive tone testing pattern in other 1cm×1cm square. The shoot area of the e-beam was set as a 1μm×1μm square for writing the positive resist and negative resist. As indicate from Figure 3-7 (b), E₂ exposure was used to transfer the zwitterresist from positive to negative tone, and the shoot area of E₂ exposure for zwitterresist was set as 4 μm× 4 μm square. The writing rate of the e-beam depended on the shoot area, and the writing rate used in zwitterresist was faster than the writing rate used for positive and negative tones. The result in Figure 3-7 (a) suggested that the throughout of zwitterreist was faster than that of the negative tone for pattern number below 500000 and faster than that of a positive tone for pattern number below about 300000.

3.4 CONCLUSIONS

The positive resist is affected by high electron doses ($>300 \mu\text{C}/\text{cm}^2$), and the resist changes into that with a negative tone. In the outer region, the scattering dose remains in the range of 3–300 $\mu\text{C}/\text{cm}^2$. The simultaneous demonstration of positive tone and negative tone leads to the formation of a ring pattern. The natural logarithm

dependence of ring width and electron beam dose is linear at 300– 550 $\mu\text{C}/\text{cm}^2$ and 600–900 $\mu\text{C}/\text{cm}^2$, respectively. From 600 $\mu\text{C}/\text{cm}^2$, the heating effect is found in addition to the scattering effect. Taking the electron scattering and electron heating into consideration, a semi-empirical model for prediction of ring width for zwitterresist is established. The model demonstrates a very good correlation in comparison with the experimental results obtained from in-line SEM measurements.



REFERENCES

1. R. N. Castellano: *Solid State Technol.* **45** (2002) 44.
2. Semiconductor Industry Association, International Technology Roadmap for Semiconductor 2001 (SIA publication, Texas, 2001).
3. F. H. Ko; J. K. Chen; C. T. Pan; H. L. Chen: Proc. 46th Int. Conf. Electron, Ion and Photo Beam Technology and Nanofabrication, 46th EIPBN, 201 (2002).
4. L. F. Thompson; C. G. Wilson; M. J. Bowden. Introduction to Microlithography (ACS publications, Washington DC, 1994) Chap 2.



Table 3-1. Results of scattering and heating coefficients for α_s , α_h , $\ln K_s$ and $\ln K_h$ at various dose ranges and design radiuses.

Dose	$\leq 600 \mu\text{C}/\text{cm}^2$		$> 600 \mu\text{C}/\text{cm}^2$	
Design radius (r_1)	1–50 (μm)	100–10000 (μm)	1–50 (μm)	100–10000 (μm)
α_s	0.15	0.25	0.15	0.25
$\ln K_s$	$0.23 \ln r_1 - 0.74$	$0.24 \ln r_1 - 1.38$	$0.23 \ln r_1 - 0.74$	$0.24 \ln r_1 - 1.38$
α_h	0	0	$0.1 + 0.05 \ln r_1$	$0.1 + 0.05 \ln r_1$
$\ln K_h$	0	0	$-0.13 \ln r_1 - 1.16$	$-0.13 \ln r_1 - 1.16$
Ring width model	(I)	(II)	(III)	(IV)

(I) $\ln D = (0.15) \ln E + (0.23 \ln r_1 - 0.74)$, (II) $\ln D = (0.25) \ln E + (0.24 \ln r_1 - 1.38)$

(III) $\ln D = (0.25 + 0.05 \ln r_1) \ln E + (0.1 \ln r_1 - 1.9)$, (IV) $\ln D = (0.35 + 0.05 \ln r_1) \ln E + (0.11 \ln r_1 - 2.54)$



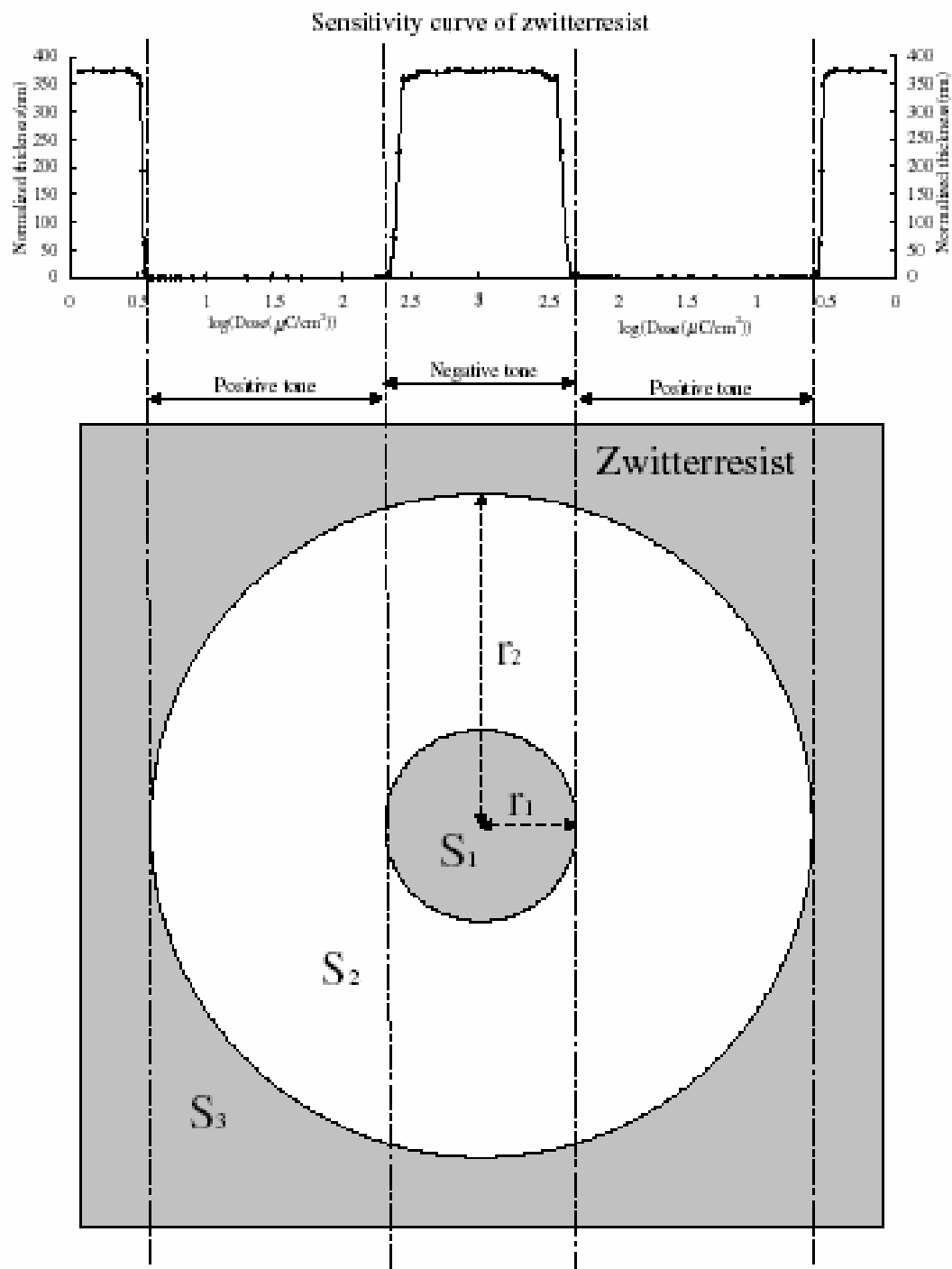
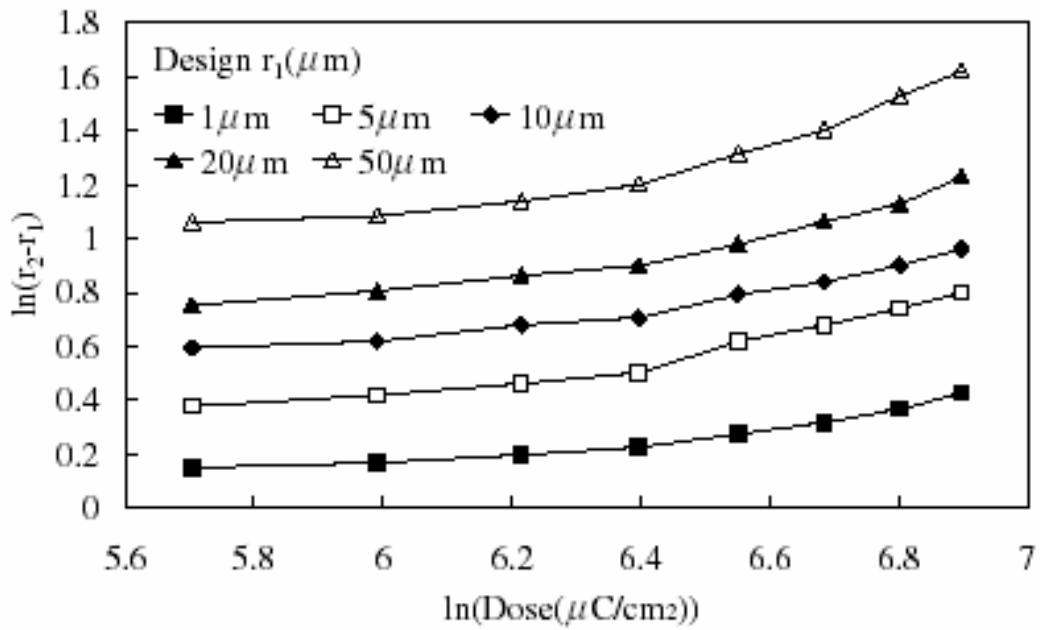
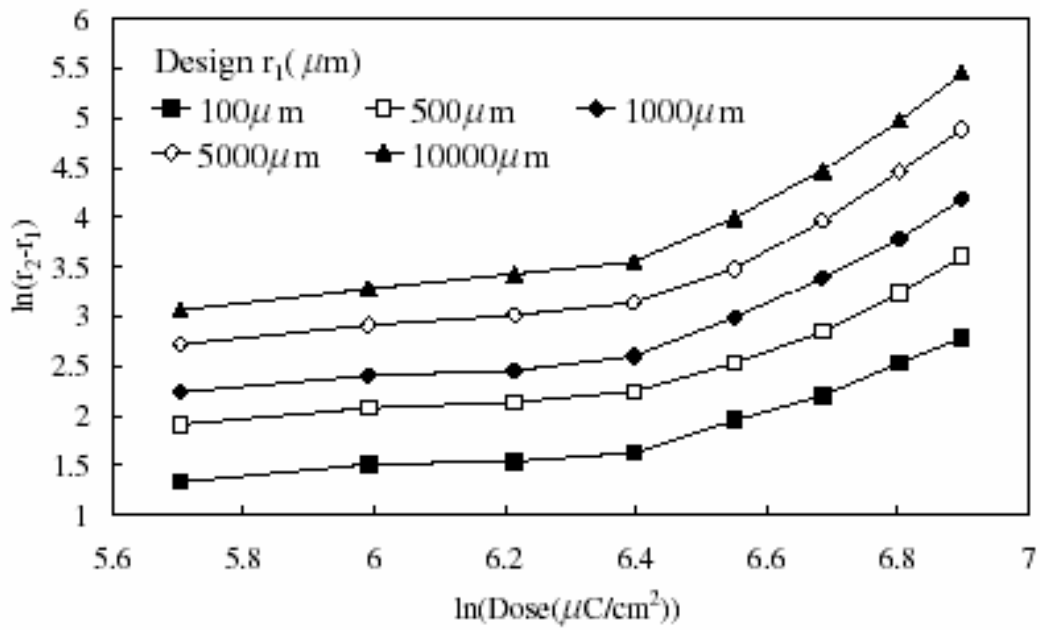


Figure 3-2. Sensitivity curve of zwitterresist and formation of ring pattern on zwitterresist.



(a)



(b)

Figure 3-3. Effect of electron beam dose on ring width at design r_1 of (a) 1 mm to 50 mm, and (b) 100 mm to 10000 mm.

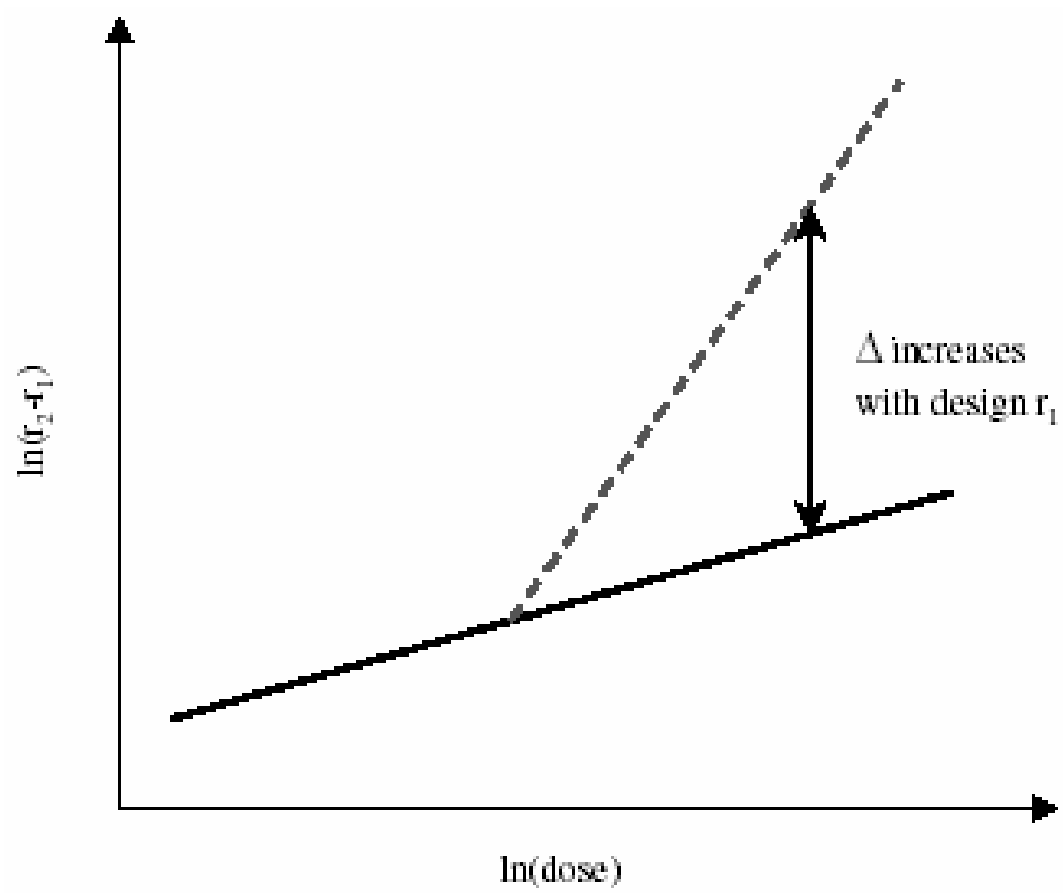


Figure 3-4. Electron scattering effect (in solid line) and the electron heating effect (dashed line).

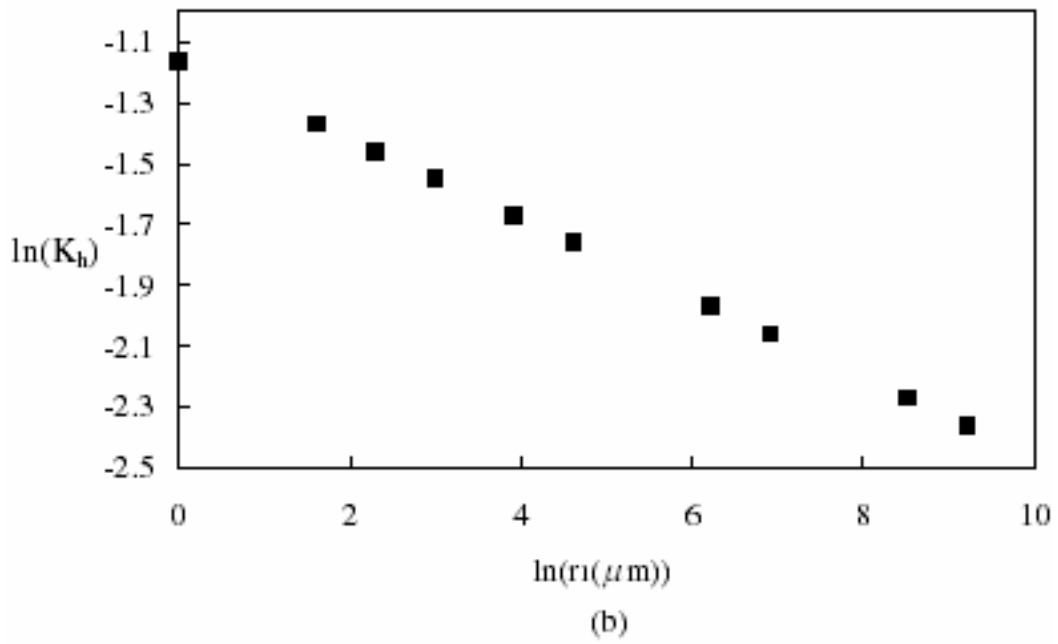
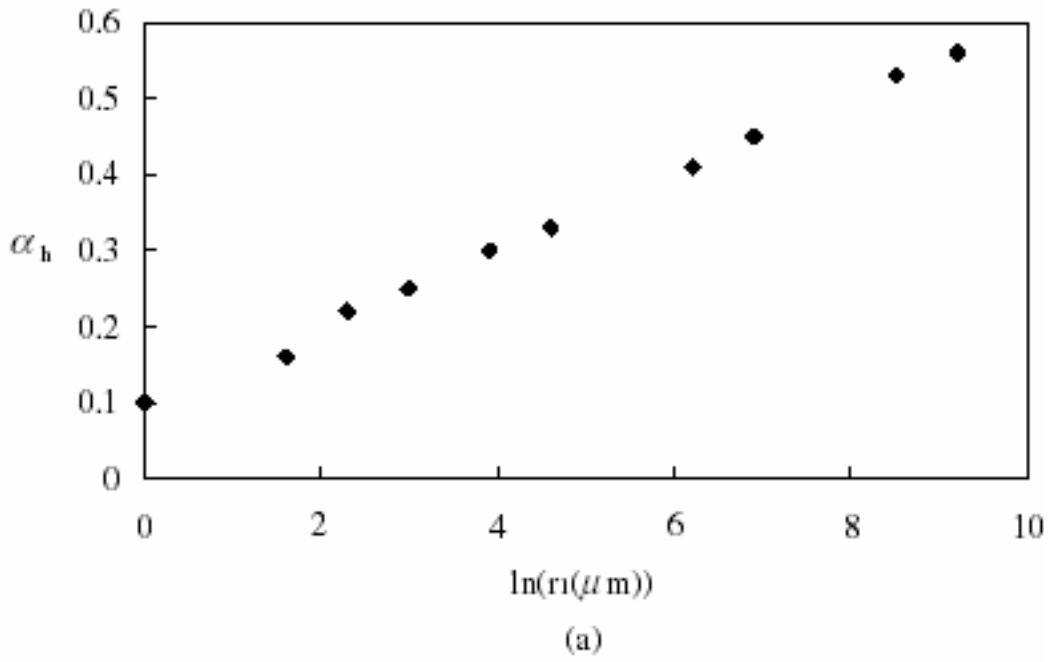


Figure 3-5. Relationship of electron heating coefficients (a) α_h and (b) $\ln K_h$ with design radius.

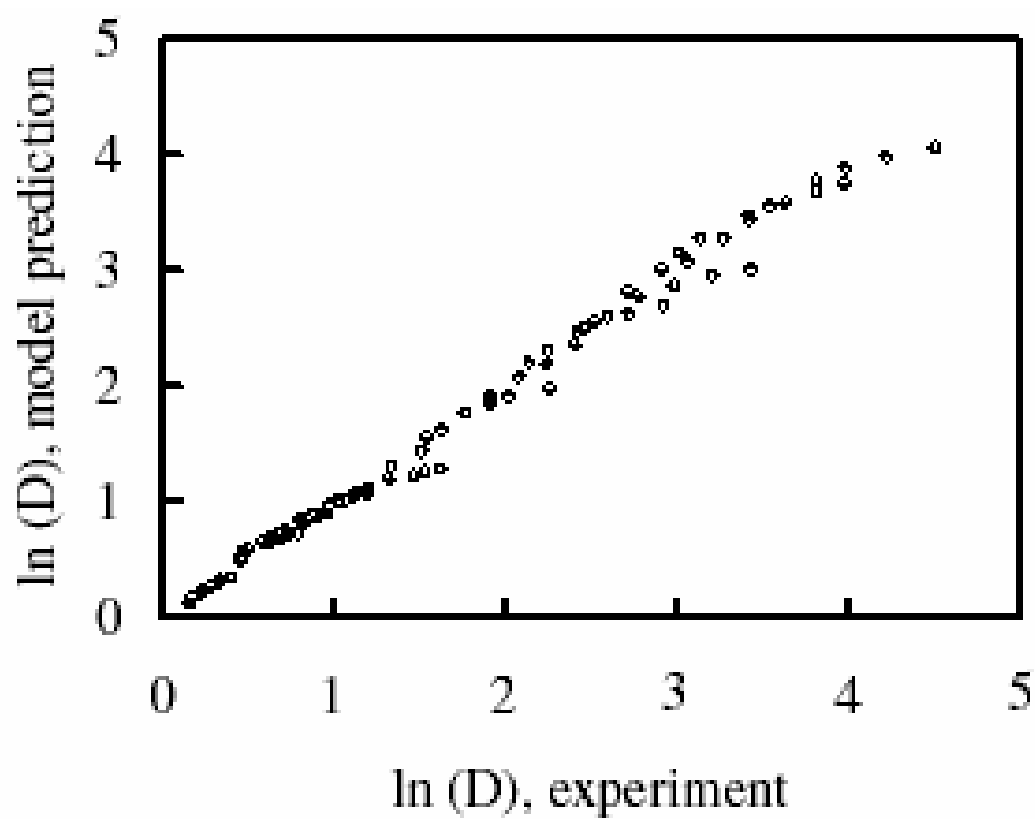
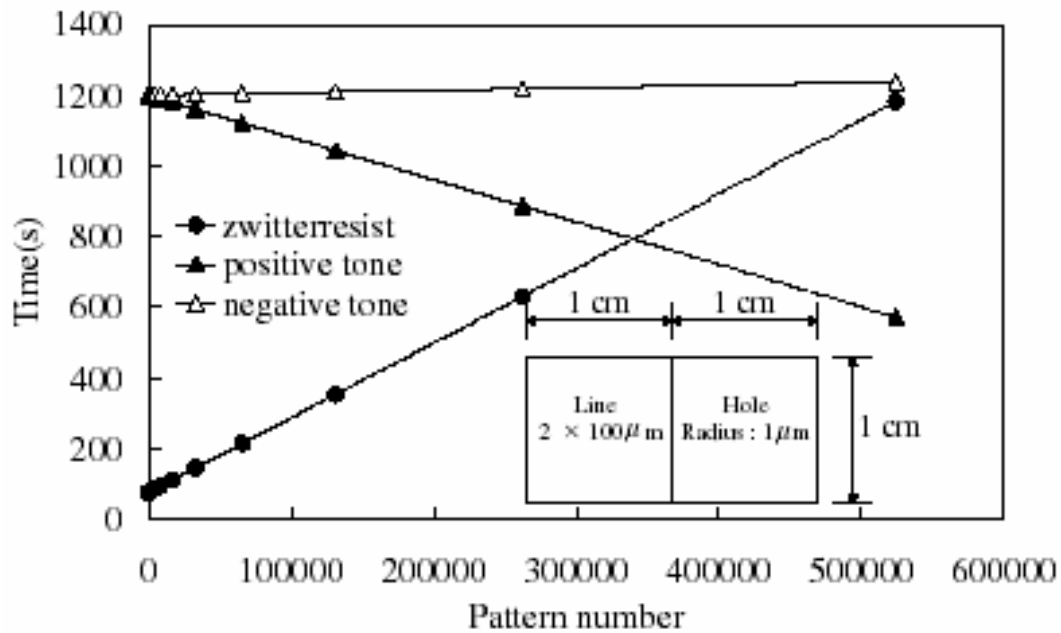
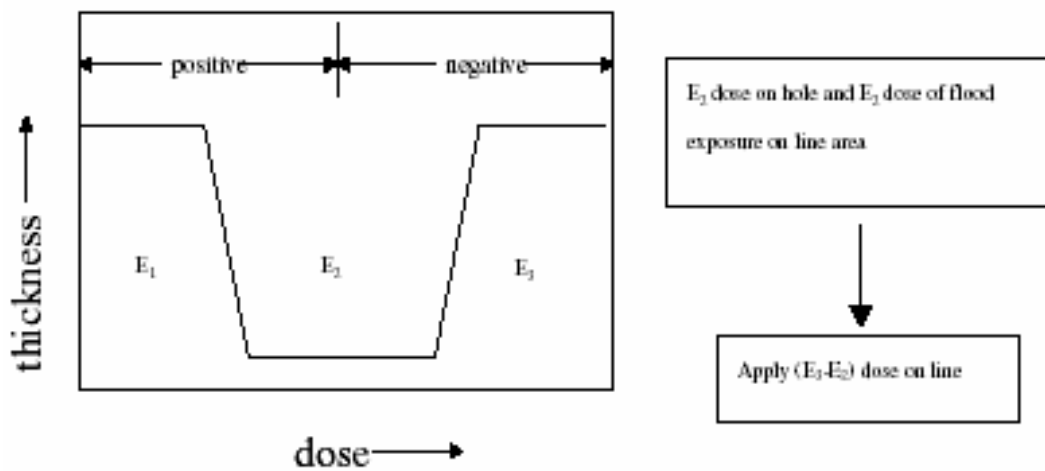


Figure 3-6. Comparison of ring width obtained from experimental data and model prediction.



(a)



(b)

Figure 3-7. (a) Effect of pattern number (pattern number of 500 means 500 lines and 500 holes) for writing time. The evaluation area is shown in the inset. The dose for positive resist is $15 \mu\text{C}/\text{cm}^2$. The dose for negative resist is $15 \mu\text{C}/\text{cm}^2$. (b) Dose strategy for zwitterresist is on the right hand side. E_2 is $5 \mu\text{C}/\text{cm}^2$, and E_3 is $600 \mu\text{C}/\text{cm}^2$.